Behaviour of the Faujasite Zeolite Occluded with Ti(IV) and Zr(IV) and its Interaction with Nickel Hexacyanoferrate (III): A Comparative Study in the Voltammetric Detection of Isoniazid

Maiara de Souza Magossi[a], Murilo Santos Peixoto[a], Abner Santos Baroni[a],

Alexssandro dos Santos Felipe[a], Newton Luiz Dias Filho[a], Fábio Simões de Vicente[b],

Devaney Ribeiro do Carmo[a] *

*[a]Universidade Estadual Paulista (UNESP), Faculdade de Engenharia,
Departamento de Física e Química, Av. Brasil, 56, 15385-000, Ilha Solteira, SP, Brasil.
[b]Universidade Estadual Paulista (UNESP), Instituto de Geociências e Ciências Exatas,
Departamento de Física, Av. 24-A, 1515, 13506-900, Rio Claro, SP, Brasil.*

This study describes titanium and zirconium incorporations into a FAU zeolite and subsequent modification with nickel hexacyanoferrate.The obtained materials (ZTiNiH and ZZrNiH) were characterized by Fourier Transform Infrared Spectroscopy (FTIR), Scanning Electron Microscopy (SEM), X-ray Dispersive Energy Spectroscopy (EDS), Porosity and Surface Area and Cyclic Voltammetry (CV). The cyclic voltammograms of the modified ZTiNiH and ZZrNiH carbon paste electrodes in the proportions graphite-modifier (20% m/m) indicate sensitivity to isoniazid (IZN). The modified ZTiNiH carbon paste electrode displayed a linear analytical curve response from 4.0×10^{-5} to 7.0×10^{-4} mol L^{-1} and a limit of detection of 4.9×10^{-5} mol L^{-1}, while the modified ZZrNiH electrode presented a linear analytical curve response from 1.0×10^{-5} a 3.0×10^{-4} mol L^{-1} and a limit of detection of 2.0×10^{-5} mol L^{-1}. The amperometric sensitivity was 47.59 mA/mol L^{-1} and 20.55 mA/mol L^{-1} for ZTiNiH and ZZrNiH respectively. After catalytic IZN electro-oxidation, a study concerning the main IZN interferents was performed and its recovery from a synthetic urine sample was assessed. The obtained ZTiNiH and ZZrNiH materials are noteworthy for their good limit of detection and recovery eficiency when applied to real samples, thus comprising potential candidates for the development of electrochemical sensors aiming at IZN detection.

Keyword: *Zeolite, Nickel hexacyanoferrate, Isoniazid, Cyclic voltammetry.*

1. Introduction

Zeolites comprise several natural and synthetic minerals that share common characteristics. These compounds consist of aluminosilicates presenting a three-dimensional crystal lattice composed of TO$_4$ tetrahedrons, where the "T" can be Al, Si, Ga, Ge, among others. The most common elements are Si (IV) and Al (III), linked by an oxygen atom. Due to their cavities and channels, zeolites display an extremely large internal surface area compared to their external surface[1-3]. They also present a microporous structure, forming a system of channels and cavities of uniform pore dimensions, displaying ion exchange capacity, high thermal stability and adsorption capacity, as well as the capability to create catalytic sites and a complex network of channels that allows for different types of selectivity. Because of this, zeolites can be applied in varied fields, such as in catalysis[4,5], electrocatalysis[6,7], metal adsorption from wastewater and soil[8-10] and as heterogeneous catalysts in the petrochemical industry[11-13], among others.

Zeolites belonging to the faujasite family are known as zeolite X, presenting Si/Al ratios between 1.0 and 1.5, and zeolite Y, with Si/Al ratios greater than 1.5. In the present study, titanium and zirconium were incorporated into zeolite Y (Na-FAU-Si/Al 2.5) for the catalytic electro-oxidation of isonicotinic acid or 4-pyridinecarboxylic acid, commercially known as isoniazid (IZN) and its chemical structure is illustrated by Figure 1.

When associated with rifampicin, IZN is widely employed in the prevention and treatment of tuberculosis, displaying bacteriostatic and bactericidal action and interfering with the metabolism of nucleic acids, bacterial proteins, carbohydrates, and lipids[14,15]. However, high IZN concentrations can lead to intoxication, infammation, loss of liver function, epilepsy and even death when administered in long-term therapies. Thus, IZN determinations in biological fuids are extremely important for therapeutic control, requiring quick, sensitive and selective quantitative IZN determination methods in biological fuids[16,17]. In this regard, several analytical methods have been developed for IZN quantification in biological samples, including high performance liquid chromatography[18], capillary electrophoresis[19], fuorimetry[20], chemiluminescence[21], spectrophotometry[22] and voltammetric methods[23,24].
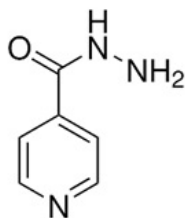
Figure 1. Chemical structure of Isoniazide (IZN).

In this work we will comparatively discuss the synthesis and properties of a zeolite of the type Faujasite occluded with Ti and Zr containing on its surface an electroactive transition complex for the detection of isoniazid using a carbon paste electrode.

Carbon paste electrodes (CPE) are made from carbon powder (graphite) and a chemically inert binder, usually mineral oil. The working electrode is prepared by mixing the modifier and paste in defined proportions. They are conductors and have low capacitive current and are especially suitable for preparing modified electrodes and can be used with mixtures of different modifiers, aiming to obtain pre-determined properties[25,26]. These electrodes are simple to prepare and offer an easily renewable surface, but their practical applicability is limited as they require the individual to have considerable experience in this process. In contrast to solid, disposable electrodes that are commercially produced and are reproducible, the carbon paste electrode can differ from one preparation to another[25,26].

In the treatment of tuberculosis, isoniazid (pyridine-4-carboxylic acid hydrazide) is one of the most effective agents. It is usually prescribed in order to prevent the development of clinical tuberculosis[27]. The action of isoniazid may be either bacteriostatic or bacteriocidal, depending on the concentration of the drug attained at the site of infection and the susceptibility of the infecting organism to the drug. In some cases, overdosing on isoniazid has resulted in poisoning accidents, including death[28]. As a result, controlling the level of isoniazid in human body fluids is an extremely important aspect of clinical chemistry. In contrast, due to the small concentration difference between effective therapeutic and toxic dosage levels, it is important to develop a rapid and specific method for determining the level of isoniazid in body fluids to facilitate the diagnosis of isoniazid intoxication. Due to the advantages of simplicity, practicality, excellent reproducibility, good stability, low cost, and real-time detection of isoniazid, voltammetric methods have been widely used to detect isoniazid. Therefore, it is an extremely useful technique for detecting environmental pollutants[29] and determining drugs and organic compounds in real-time samples[30-33]. In addition, voltammetric methods, in particular, display several advantages, such as simplicity, practicality, low cost and real-time detection.

2. Experimental

2.1. Reagents and solutions

The Faujasite type zeolite (FAU), Isoniazid, graphite (15-20 μm) and potassium hexacyanoferrate (III) were purchased from Sigma-Aldrich and all others reagents used in this work were analytical grade (Reagen, Nuclear, Vetec, Dinâmica) and were used without further purification. All solutions were prepared using deionized water with resistivity of not less than 18.2 MΩ cm (Milli-Q system,). Isoniazid solutions were prepared immediately prior do use.

2.2. Zeolite inorganofunctionalization with Ti(IV) and Zr(IV)

The organofunctionalization of the FAU zeolite with Ti(IV) and Zr(IV) was performed according to Magossi et.[27]. A total of 40m L of tetrahydrofuran (THF), 500 mg of zeolite, 1.0×10^{-3} mol (1.0mL) of titanium isopropoxide and 1.0×10^{-3} mol (1.0 mL) of zirconium propoxide were used and the obtained materials were termed ZTi and ZZr.

2.3. Nickel hexacyanoferrate formation on ZTi and ZZr furfaces

The formation of nickel hexacyanoferrate on the ZTi and ZZr surfaces through the same synthesis route was carried out according to Magossi et al.[27]. A total of 200 mg of ZTi and ZZr, 50 mL of an aqueous nickel chloride solution $(1.0 \times 10^{-3}$ mol L$^{-1})$ and 50 mL of potassium hexacyanoferrate (III) $(5.0 \times 10^{-3}$ mol L$^{-1})$ were used. The materials were stored in the dark and named ZTiNiH and ZZrNiH.

2.4. Techniques

2.4.1. Fourier transform infrared spectra

The vibrational spectra of the obtained materials were determined according to Magossi et al.[28] employing a Nicolet 5DXB FTIR spectrometer. The samples were analyzed at the Ilha Solteira Physics and Chemistry Department (UNESP), Brazil.

2.4.2. Scanning Electron Microscopy (SEM) and XRay Dispersive Energy Spectroscopy (EDS)

The obtained materials were analyzed employing a Carl Zeiss EVO LS15 scanning electron microscope coupled to an EDS. The samples were analyzed in powder form at the Ilha Solteira Physics and Chemistry Department (UNESP), Brazil.

2.4.3. Porosity and surface area

The material surface areas and porosities were assessed according to Magossi et al.[27] employing a Micromeritics ASAP 2010 pore analyzer.

2.4.4. Voltammetric study

Electrochemical measurements were performed employing an Autolab PGSTAT 128 N Potentiostat. The electrochemical system comprised a three-electrode cell, a modifed carbon paste working electrode, a reference electrode Ag|AgCl|KCl(sat) and a platinum auxiliary electrode. All electrochemical measurements were performed at room temperature

3. Results and Discussion

3.1. Fourier Transform Infrared Spectra

The Fourier transform infrared spectra of the FAU zeolite matrix and the ZTi and ZZr materials are depicted in Figures 2A, 2B and 2C, respectively.
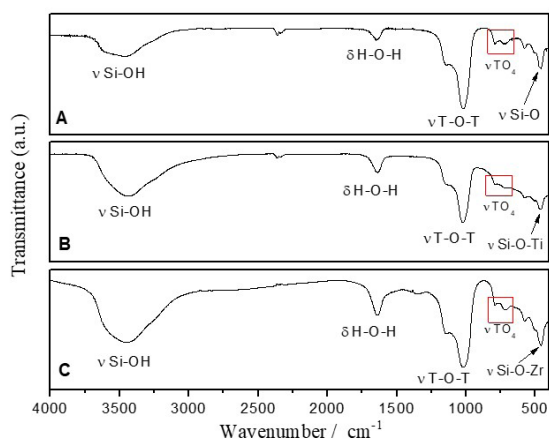
Behaviour of the Faujasite Zeolite Occluded with Ti(IV) and Zr(IV) and its Interaction with Nickel
Hexacyanoferrate (III): A Comparative Study in the Voltammetric Detection of Isoniazid

3

Figure 2. Vibrational spectra in the infrared region for (A) FAU Zeolite; (B) ZTi and (C) ZZr.

The FAU zeolite spectrum (Figure 2A) presented absorption bands at 3510 and 1640 cm^{-1}, indicating the presence of silanol groups, as well as physically adsorbed water molecules. An intense vibration band at 1025 cm^{-1} was also noted, attributed to the asymmetric stretching of T-O-T bonds, characteristic of zeolites, where T represents the tetrahedrally coordinated silicon and aluminum atoms, that is, TO_4 (T = Si or Al). The bands at 790 and 728 cm^{-1} correspond to vibrations external to the TO_4 tetrahedra, due to symmetrical stretching. An absorption band present at 576 cm^{-1} is characteristic of FAU zeolite structural rings (D6R), while an absorption band at 460 cm^{-1} can be attributed to T-O bond bending[34,35].

Figures 2B and 2C depict the ZTi and ZZr spectra, respectively. Characteristic FAU zeolite matrix bands were observed, as well as absorption bands at 459 and 456 cm^{−1}, attributed to T-O bond vibrations (T = Al or Si) containing titanium and zirconium atoms, respectively[36].

Figure 3 illustrates the vibrational spectra obtained for potassium hexacyanoferrate(III) (A, ZTiNiH (B) and ZZrNiH (C), respectively. Bands corresponding to the FAU zeolite structure and at 2169 and 2103 cm^{-1} were observed for ZTiNiH and ZZrNiH (Figure 3B and 3C), attributed to C≡N stretching[37,38], evidencing complex formation.

3.2. Scanning Electron Microscopy and XRay Dispersive Energy Spectroscopy

Figure 4 illustrates the micrographs for (A) the FAU zeolite, (B) ZTi and (C) ZZr at 20.000X magnification, respectively. Particle clusters of varying sizes were observed in the FAU zeolite, ranging from about 660 to 860 nm. After Ti and Zr incorporation into the FAU zeolite matrix, larger particle agglomerations were observed in relation to its precursor, suggesting inorganofunctionalization FAU zeolite morphological influence[39].

The micrographs for (A) ZTiNiH and (B) ZZrNiH at 20.000X magnification displayed in Figure 5 indicate particle agglomeration topology changes following the applied chemical reactions.

The EDS spectra of the FAU zeolite samples, namely (A), ZTi (B), ZZr (C), ZTiNiH (D) and ZZrNiH (E), are presented
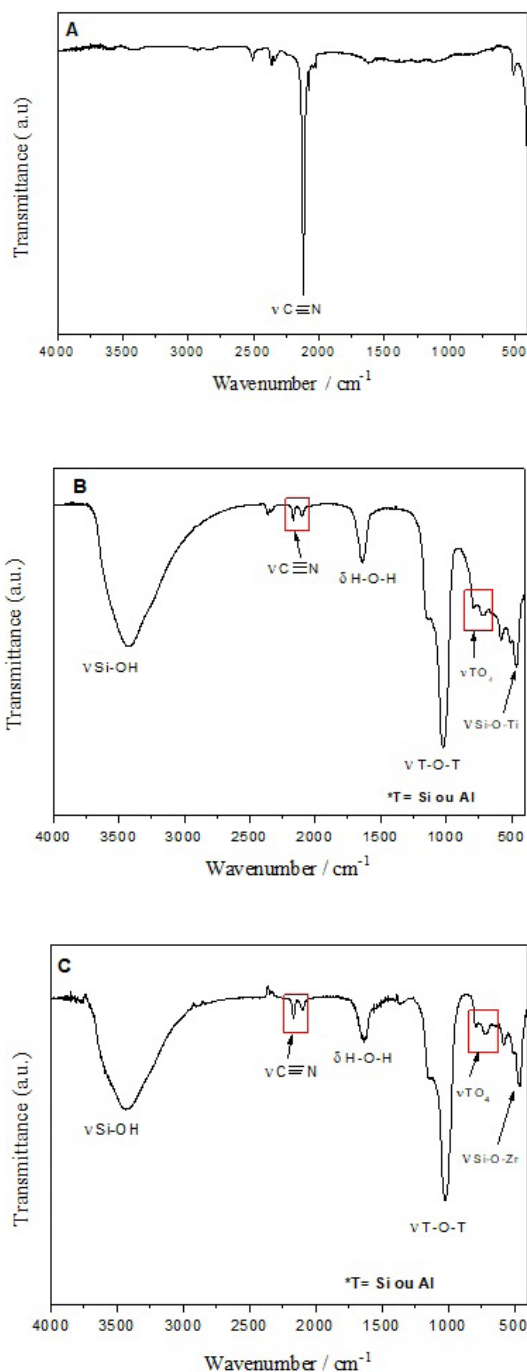

Figure 3. Vibrational spectra in the infrared region for (A) Potassium hexacyanoferrate(III), (B) ZTiNiH and (C) ZZrNiH.

in Figure 6. The presence of silicon, oxygen, aluminum, titanium and zirconium, all characteristic of FAU zeolites and modifiers, are observed, reinforcing matrix Ti and Zr incorporation. Nickel, iron and potassium were also detected in the obtained materials subsequently to the interaction of the ZTi and ZZr precursors with potassium Ni (II) and hexacyanoferrate (III), as expected following successful reactions and material matrix adsorption. The qualitative composition of the material elements determined by EDS is displayed in Table 1, in agreement with the FTIR results.
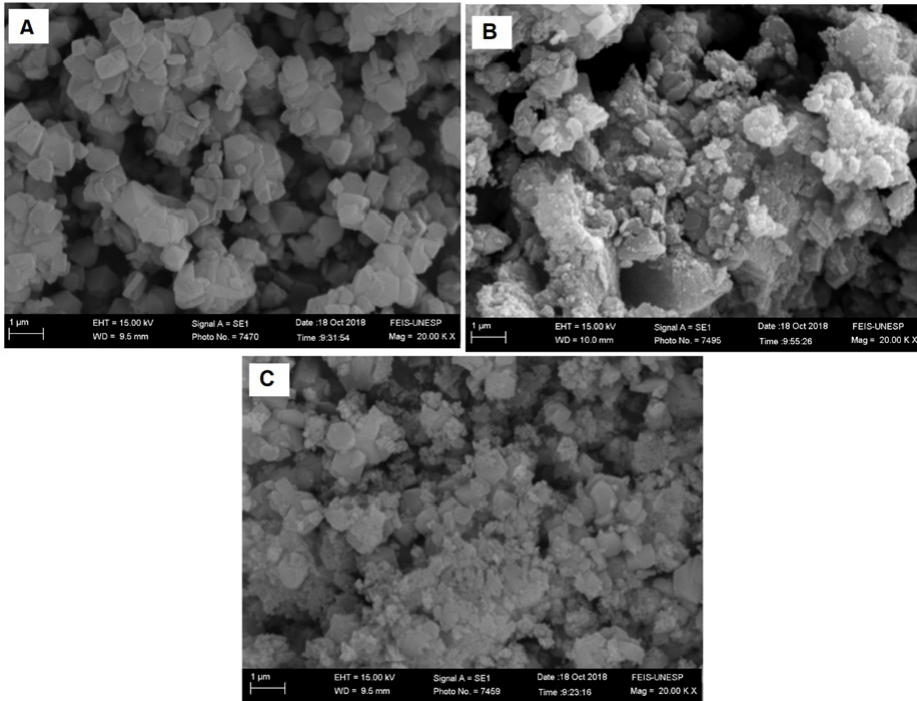
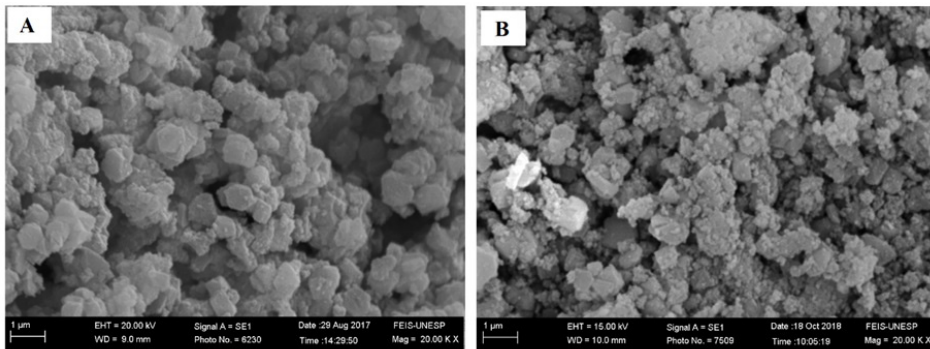**Figure 4.** SEM at 20.000X for (A) FAU Zeolite; (B) ZTi and (C) ZZr.

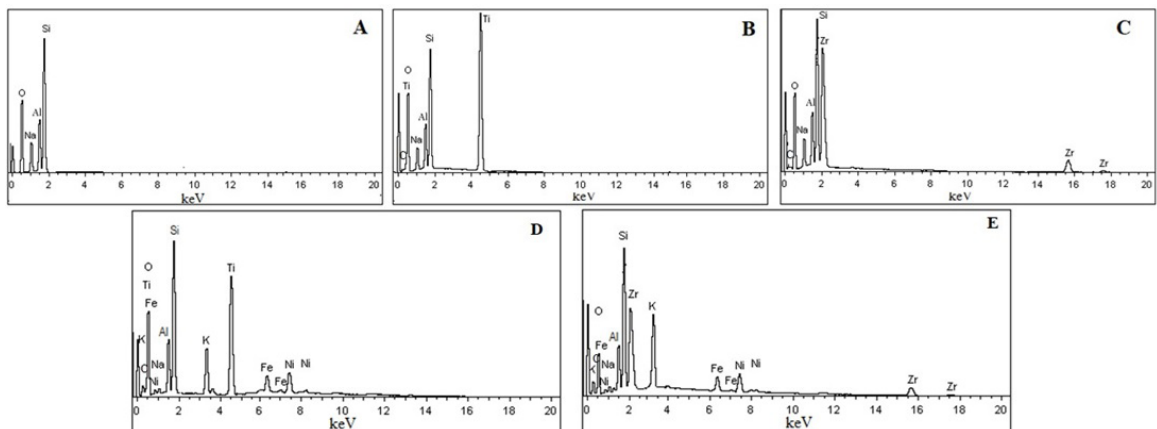**Figure 5.** SEM images at 20.000X magnification for (A) ZTiNiH and (B) ZZrNiH.

Figure 6. X-ray Dispersive Energy Spectra for (A) the FAU Zeolite, (B) ZTi, (C) ZZr, (D) ZTiNiH and (E) ZZrNiH.

Behaviour of the Faujasite Zeolite Occluded with Ti(IV) and Zr(IV) and its Interaction with Nickel
Hexacyanoferrate (III): A Comparative Study in the Voltammetric Detection of Isoniazid

5

Table 1. Elemental composition of the obtained materials determined by EDS.

Material	Semi-quantitative composition (% at.)									
	C	Na	O	Si	Al	Ti	Zr	Ni	Fe	K
FAU Zeolite	----	7.66	74.18	12.57	5.59	-	-	-	-	-
ZTi	18.66	2.19	69.03	4.29	1.93	3.90	-	-	-	-
ZZr	37.90	1.97	53.11	3.55	1.47	-	2.0	-	-	-
ZTiNiH	16.30	0.79	70.00	4.53	2.10	3.03	-	1.02	1.05	1.08
ZZrNiH	32.30	0.71	55.24	3.40	1.92	-	2.10	1.31	1.20	1.82

3.3. Porosity and surface area

Figure 7 illustrates the N$_2$ adsorption-desorption displaying type I and II isotherms combinations with a type H4 hysteresis[40] for (A) the FAU zeolite, (B) ZTi, and (C) ZZr.

An accentuated N$_2$ adsorption at low relative pressure (p/p^0) was observed, generally detected in materials with more pronounced adsorption at low pressure, associated with micropore filling, both frequently found in zeolites[4,40]. Also a broadening of the hysteresis loop in the range of relative pressures from 0.5 to 1.0 was observed for ZTi and ZZr (Figure 7B and 7C), suggesting the formation of mesopores[4,41].

Pore size distribution graphs of the FAU zeolite and ZTi and ZZr materials, are depicted in Figure 8, indicating formation of a larger class of pores (mesopores) in ZTi and ZZr compared to FA thus confirming Ti and Zr zeolite matrix occlusion (Figure 8B and C). Table 2 lists the surface analysis parameters (surface area, pore size, and micropores/mesopores volumes) of these materials, indicating decreased ZTi and ZZr surface areas in relation to the FAU zeolite and increased pore sizes due to metal matrix incorporation.

3.4. Voltammetric study

Using the Randles-Sevcik equation[42] (Equation 1) , the effective surface area of the electrode of ZTi and ZZr immersed in a potassium ferricyanide solution of 10 mM and a potassium chloride solution of 0.5 mol L^{-1}, were calculated to be 10.6 and 7.1 mm^2 respectively.

$$I_p = \left(2.69 \times 10^5\right) n^{3/2} AD^{1/2} CV^{1/2} \qquad (1)$$

where, I$_p$ is the peak current in A. C is the concentration of the electroactive species (mol cm^{-3}), n is the number of electrons exchanged, D is the diffusion coefficient in cm^{2}s^{-1}, v is the scan rate (V s^{-1}) and A is the electroactive surface area (cm^2).

The electrochemical properties of the ZTiNiH and ZZrNiH graphite paste were investigated through cyclic voltammetry employing a potential range from 0.0 to 1.0V. The modifed pastes were prepared by mixing the obtained materials with graphite at a 20% (w/w) ratio using 20 μL of Nujol mineral oil.

It was found that the redox process of these two metal complexes in the FAU zeolite cavities was more pronounced than in the MCM-41 platform cavities[27]. In FAU zeolite, the measurement of the anodic and cathodic current intensity was more accurate and easier to calculate. In order to be used as voltammetric sensors, it is extremely imperative that these materials meet these requirements. In previous analyses of

the choice of supporting electrolyte concentration, pH, and scan rate, we selected KCl 1.0 mol L^{-1}, pH 7.0, v=20 mVs^{-1} as the optimal parameters for IZN electro-oxidation.

3.4.1. Catalytic isoniazid electrooxidation

The catalytic IZN electro-oxidation process employing the modifed ZTiNiH and ZZrNiH graphite paste electrode is illustrated in Figures 9(I). indicates that the graphite paste electrode without the modifier (A) did not present any redox pair at the applied potential range, from 0.0 to 1.0 V, in the absence of IZN, exhibiting an oxidation peak around 0.81 V in the presence of IZN (7.0×10^{-4} mol L^{-1}) under optimized conditions (B). The modified ZTiNiH graphite paste electrode presented an anodic peak at 0.56 V in the absence of isoniazid (C), increasing anodic peak current intensity in the presence of 7.0×10^{-4} mol L^{-1} of IZN with decreasing cathode peak current intensity and a 0.25 V decrease in the IZN oxidation peak, characterizing an electrocatalysis process (D). Figure 9(II) indicates a linear response from of 4.0×10^{-5} to 7.0×10^{-4} mol L^{-1} with a corresponding equation Y (μA) = 66.88 + 47.59×10^3 [IZN] and a correlation coefficient of R^2 = 0.997. The limit of detection was 4.9×10^{-5} mol L^{-1} with a relative standard deviation of ± 3% (n = 3) and amperometric sensitivity of 47.59 mA/mol L^{-1}.

The ZZrNiH material also displayed a favorable response to catalytic IZN electro-oxidation (Figure 10 (I) . In the absence of IZN (A) the graphite paste electrode did not exhibit any redox process at the applied potential range from 0.0 to 1.0 V, while in the presence of 3.0×10^{-4} mol L^{-1} IZN an oxidation peak around 0.76 V was observed (B). The modified ZZrNiH graphite paste electrod exhibited an anodic peak at 0.54 V in the absence of IZN (C), with an increase in anodic peak current intensity followed by a decrease in cathodic peak current intensity, characterizing an electrocatalysis, in the presence of 3.0×10^{-4} mol L^{-1} IZN (D). In this case, IZN oxidation decreased by 0.22 V under optimized conditions. Figure 10 (II) indicates a linear response from 1.0×10^{-5} to 3.0×10^{-4} mol L^{-1} with a corresponding equation Y (μA) = 21.08 + 20.55×10^3 [IZN] and a correlation coefficient R^2 = 0.998. The limit of detection was 2.0×10^{-5} mol L^{-1} with a relative standard deviation of ± 2% (n = 3) and amperometric sensitivity of 20.55 mA/mol L^{-1}.

The proportional increase in the intensity of the anodic peak current (Ipa) is due to the electrocatalytic IZN oxidation in both mat3rials (ZTiNiH and ZZrNiH), comprising two steps, one electrochemical (E.E.) and another chemical (E.Q.), represented by Equations 2 and 3, respectively. The process occurs as described by Magossi et al.[27]
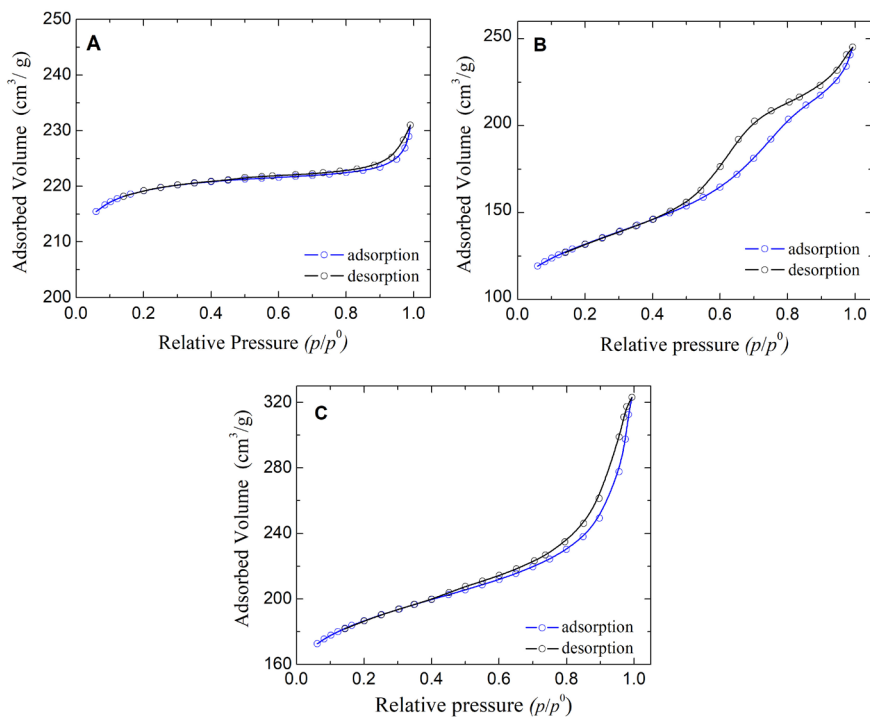
Figure 7. Nitrogen adsorption–desorption isotherms for (A) the FAU zeolite, (B) ZTi and (C) ZZr.
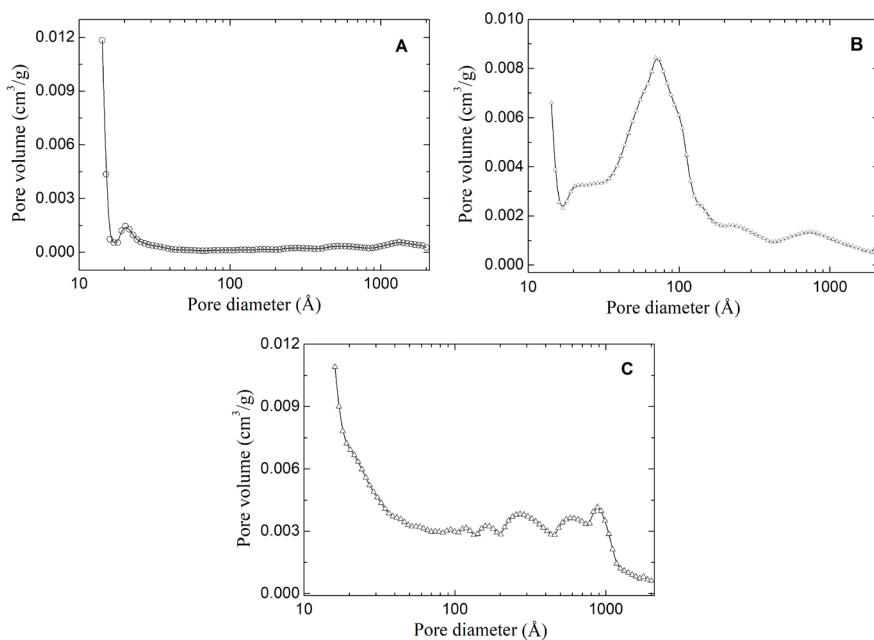

Figure 8. Pore size distribution graphs for (A) the FAU zeolite, (B) ZTi and (C) ZZr. Acording to IUPAC[40], *micropores* are $\leq$ 20 Å, and *mesopores* between 20 and 500 Å.

Table 2. Surface parameters for the FAU zeolite, ZTi, and ZZr samples from the nitrogen adsorption isotherms. *Micropore(micro)* and *mesopore* (*meso*) volumes are indicated related to the total pore volume.

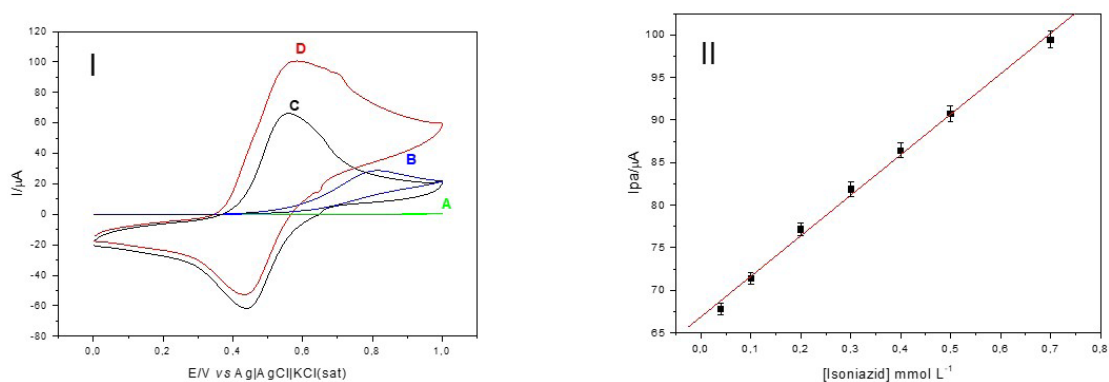| Sample	Surface area, S_{BET} (m^2/g)	Mean pore size, l_p (Å)	Pore volume, V_p (cm^3/g) (total / micro / meso)
Zeolite	744	20	0.360 / 0.310 / 0.060
ZTi	452	60	0.372 / 0.122 / 0.250
ZZr	640	30 and 400	0.484/ 0.198 / 0.286

Figure 9. (I) Cyclic voltammograms for the (A) graphite paste electrode, (B) graphite paste electrode in the presence of 7.0×10^{-4} mol L^{-1} isoniazid, (C) modified ZTiNiH graphite paste electrode in the absence of isoniazid and (D) modified ZTiNiH graphite paste electrode in the presence of 7.0×10^{-4} mol L^{-1} isoniazid.fig. (II) Analytical curve for anodic peak currents as a function of isoniazid concentrations employing the graphite paste electrode modified with ZTiNiH (20% w/w, KCl 1.0 mol L^{-1}, pH 7.0, v = 20 mV s^{-1}).
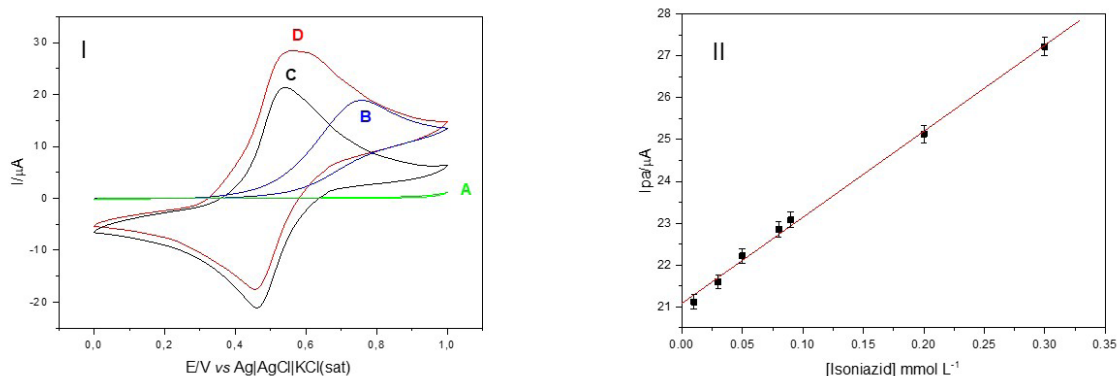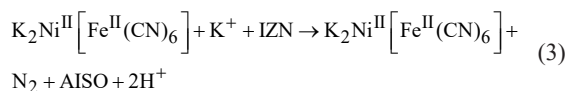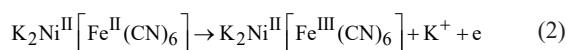

Figure 10. (I) Cyclic voltammograms for the (A) carbon paste electrode, (B) carbon paste electrode in the presence of 3.0×10^{-4} mol L^{-1} isoniazid, (C) modified ZZrNiH carbon paste electrode in the absence of isoniazid and (D) modified ZZrNiH carbon paste electrode in the presence of 3.0×10^{-4} mol L^{-1} isoniazid. (II) Analytical curve for anodic peak currents as a function of IZN concentrations employing the modified ZZrNiH carbon paste electrode (20% w/w, KCl 1.0 mol L^{-1}, pH 7.0, v = 20 mV s^{-1}).

$$K_2Ni^{II}\left[Fe^{II}(CN)_6\right] \rightarrow K_2Ni^{II}\left[Fe^{III}(CN)_6\right] + K^+ + e \qquad (2)$$

$$K_2Ni^{II}\left[Fe^{II}(CN)_6\right] + K^+ + IZN \rightarrow K_2Ni^{II}\left[Fe^{II}(CN)_6\right] + N_2 + AISO + 2H^+ \qquad (3)$$

where: IZN= isoniazid and AISO = isonicotinic acid.

The modified ZTiNiH and ZZrNiH graphite paste electrodes were shown to be close to the electrodes used in the electrocatalytic detection of IZN described in the literature[35-40], indicating they can be used to detect this compound.

The modified ZTiNiH and ZZrNiH graphite paste electrodes were shown to be close to the electrodes used in the electrocatalytic detection of IZN described in the literature, indicating they can be used to detect this compound. Table 3 lists the analytical parameters described in the literature for other electrodes used in the electrocatalytic detection of isoniazid.

Table 3. Comparison of analytical parameters described in the literature for detection isoniazid.

Systems	Concentration Range (mol L^{-1})	LOD* (mol L^{-1})	Ref.
Glassy carbon /Rh	7.0×10^{-5}–1.3×10^{-3}	1.30×10^{-5}	[39]
Glassy carbon /poly eriochrome black T (EBT)	2.9×10^{-5}–1.67×10^{-3}	1.64×10^{-5}	[42]
Pencil electrode	8.6×10^{-5}–1.37×10^{-3}	6.6×10^{-5}	[43]
Carbon paste electrode (GPE)	4.0×10^{-5}–1.0×10^{-3}	2.47×10^{-5}	[44]
Screen Printed	1.0×10^{-7}–4.6×10^{-6}	6.4×10^{-5}	[45]
Screen Printed	2.5×10^{-5}–2.0×10^{-4}	4.7×10^{-5}	[46]
Graphite Paste /ZTiHNi	4.0×10^{-5}–7.0×10^{-4}	4.9×10^{-5}	This work
Graphite Paste /ZZrHNi	1.0×10^{-5}–3.0×10^{-4}	2.0×10^{-5}	This work

3.4.2. Isoniazid interference studies and real sample determinations

The effect of IZN's main interferents (ascorbic acid, dopamine, and sucrose)[14] was evaluated by cyclic voltammetry

following the addition of aliquots of a mixed solution of these substances, as described by Magossi et al.[27]. A comparison of the effects of the main interferences (ascorbic acid, dopamine and sucrose) on the detection of isoniazid based on the ZTiNiH and ZZrNiH materials is shown in Figures 11 and 12. A substantial increase in the current intensity of the anodic current was observed at concentrations equal to or greater than 100 mol L^{-1} of interferents simultaneously with the appearance of a well-defined redox couple, likely as a result of the strong adsorption of ascorbic acid, mainly dopamine, in the graphite paste surface. This behavior was also verified
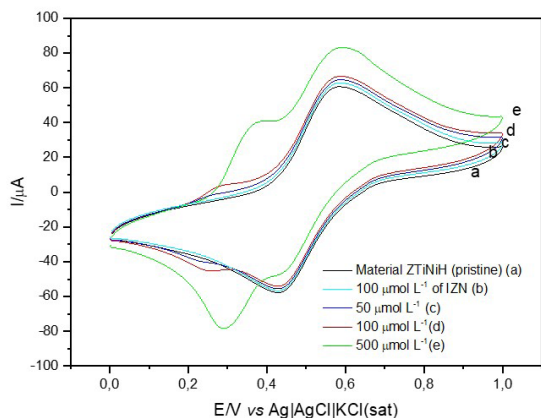
on the MCM-41 platform containing the same complexes but with less intensity[27].

The analytical performances of the modified ZTiNiH and ZZrNiH graphite paste electrodes were also investigated concerning potential application as electrochemical sensors in the determination of IZN in a synthetic urine sample, employing the addition and recovery method (spike method) and CV. The results were satisfactory, indicating good IZN recovery percentage as shown by Figure 13 and Tables 4 and 5

Table 4. Ascorbic acid, dopamine, and sucrose interferences in the presence of 100 µmol L^{-1} isoniazid employing a modified ZTiNiH graphite paste electrode (20% w/w, KCl 1.0 mol L^{-1}, pH 7.0).

Interferent species*	Concentration (µmol L^{-1})	Interference level (%)
AA + DOP + SAC	50	3.00
AA + DOP + SAC	100	6.65
AA + DOP + SAC	500	38.24

*AA - ascorbic acid, DOP - dopamine, SAC - sucrose

Table 5. Ascorbic acid, dopamine, and sucrose interferences in the presence of 10 µmol L^{-1} isoniazid employing a modified ZZrNiH graphite paste electrode (20% w/w, KCl 1.0 mol L^{-1}, pH 7.0).

Species of interferents*	Concentration (µmol L^{-1})	Interference level (%)
AA + DOP + SAC	7	3.75
AA + DOP + SAC	10	3.88
AA + DOP + SAC	70	12.68

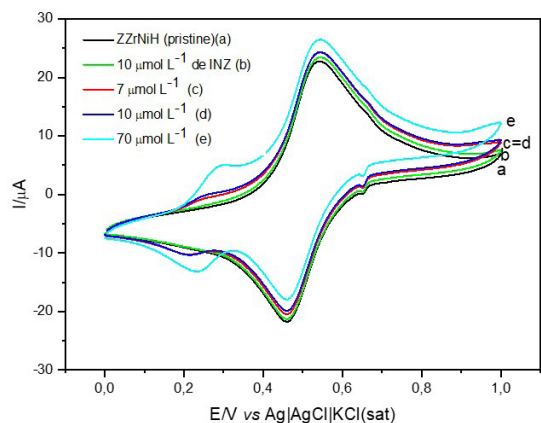*AA - ascorbic acid, DOP - dopamine, SAC - sucrose

Figure 11. Cyclic voltammograms obtained for the carbon paste electrode modified with ZTiNiH in the presence of different concentrations of a mixed solution containing ascorbic acid, dopamine and sucrose in the presence of 100 µmol L^{-1} of isoniazid (20% w/w; KCl 1.0 mol L^{-1}; pH 7.0; v = 20 mV s^{-1}): a) ZiTiNiH (Pristine); b) addition of 100µL Isoniazid; c) addition of 50 µL of the mixed solution containing interferents d) addition of 100 µL of the mixed solution containing interferents; e) addition of 500 µL of the mixed solution containing interferents.

Figure 12. Cyclic voltammograms obtained for the carbon paste electrode modified with ZZrNiH in the presence of different concentrations of a mixed solution containing ascorbic acid, dopamine and sucrose in the presence of 10 µmol L^{-1} of isoniazid (20% m/m; KCl 1.0 mol L^{-1}; pH 7.0; v = 20 mV s-1). a) ZiTiNiH (Pristine); b) addition of 10µL Isoniazid; c) addition of 7 µL of the mixed solution containing interferents; d) addition of 10 µL of the mixed solution containing interferents; e) addition of 70 µL of the mixed solution containing interferents.
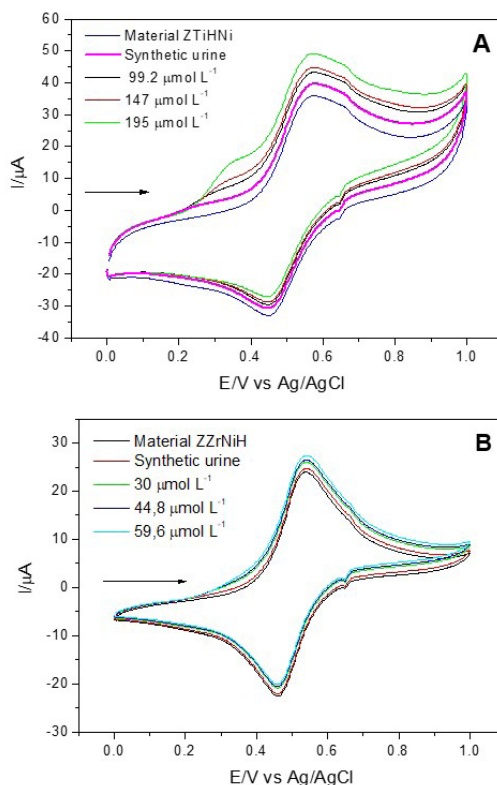

Figura 13. Cyclic voltammograms obtained related to addition-recovery studies: (A) ZTiNiH; (B) ZZrNiH (20% w/w; KCl 1.0 mol L^{-1}; pH 7.0; v = 20 mV s^{-1}).

Behaviour of the Faujasite Zeolite Occluded with Ti(IV) and Zr(IV) and its Interaction with Nickel
Hexacyanoferrate (III): A Comparative Study in the Voltammetric Detection of Isoniazid

9

(98%) and suggesting that the method reported herein is efficient and can be easily applied to IZN quantification.

Figure 13 shows the voltammograms related to the recovery studies for ZTiNiH (A) and with ZZrNiH (B) and according to the results obtained listed in Tables 6 and 7 the percentage of recovery of isoniazid obtained, were satisfactory, suggesting that the method used is efficient and can be easily applied in its determination.

3.4.3. Repeatability and reproducibility

Repeatability and reproducibility are two important parameters to evaluate the ability of a sensor Six independent modified electrodes were prepared on the same day and under the same conditions to investigate repeatability (Figure 14(A)). The electrode showed good stability and repeatability for ZTiNiH and ZZrNiH as shown by Figure 14(A) . After several measurements, showing a relative standard deviation (RSD) of 4.15% and 4.85% to ZTiNiH and ZZrNiH respectively. It was evaluated too with the same concentration of isoniazid on five consecutive days with five modified electrodes prepared independently under the same experimental conditions The reproducibility (Figure 14 (B)) in the current intensity of the anodic peak between the different electrodes was satisfactory, with a relative standard deviation of 2.04% and 3.76%. These results suggest that the ZTiNiH and ZZrNiH -modified carbon paste electrodes can be used successfully in detecting isoniazid in a real sample at millimolar level concentrations.
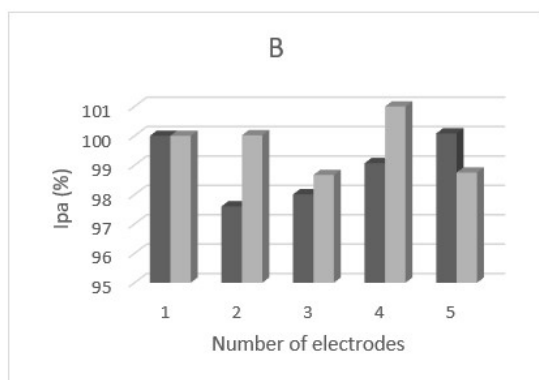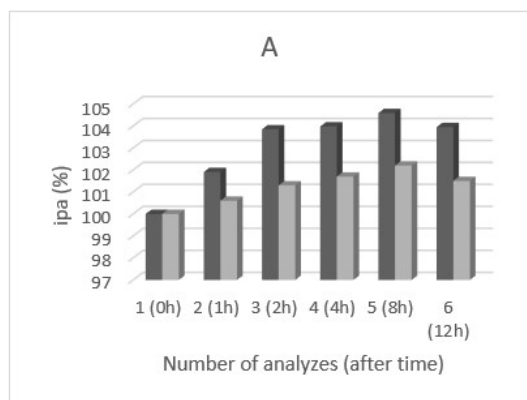

Figure 14. (A) repeatability and **(B)** reproducibility for ZTiNiH (black) and ZZrNiH (gray) (20% w/w; KCl 1.0 mol L^{-1}; pH 7.0; $v = 20mV\ s^{-1}$).

Table 6. Values obtained for determination of isoniazid in synthetic urine samples using the graphite paste electrode modified with ZTiNiH (20% w/w; KCl 1.0 mol L^{-1}; pH 7.0).

Added concentration [μmol L^{-1}]	Found concentration [μmol L^{-1}]	Recovery [%]
99.2	93	93.80
147	140	95.60
195	196	100.51

Table 7. Values obtained for determination of isoniazid in synthetic urine samples using the graphite paste electrode modified with ZZrNiH (20% m/m; KCl 1.0 mol L^{-1}; pH 7.0).

Added concentration [μmol L^{-1}]	Found concentration [μmol L^{-1}]	Recovery [%]
30	31	103.33
44.8	43.5	97.09
59.6	60.3	101.17

4. Conclusions

Titanium and zirconium have been successfully incorporated into the FAU Zeolite cavities , as demonstrated by Fourier Transform Infrared Spectroscopy, scanning electron microscopy, X-ray Dispersive Energy Spectroscopy , and Porosity and Surface Area characterizations. By subsequent chemical modification of these materials with nickel and then with potassium hexacyanoferrate(III), it was possible to obtain a material that was capable of detecting isoniazid at levels of micromolar concentrations. Cyclic voltammetry assessments indicate that the modified ZTiNiH and ZZrNiH graphite paste electrodes allow for the electrocatalytic detection of IZN with a low limit of detection. In addition, they have excellent amperometric sensitivity and recovery efficiency from synthetic samples compared to other electrodes. Thus, the ZTiNiH and ZZrNiH materials represent potential candidates for the development of an electrochemical sensor for IZN detection.

5. Acknowledgments

6. References

1. Cejka J, Bekkum HV, Corma A, Schueth F. Introduction to zeolite molecular sieves. USA: Elsevier; 2007.
2. Weitkamp J. Zeolites and catalysis. Solid State Ion. 2000;131(1-2):175-88.
3. Chica A. Zeolites: promised materials for the sustainable production of hydrogen. Int Sch Res Notices. 2013;2013:(1):907425.
4. Morales-Pacheco P, Domínguez JM, Bucio L, Alvarez F, Sedran U, Falco M. Synthesis of FAU (Y)-and MFI (ZSM5)-nanosized crystallites for catalytic cracking of 1, 3, 5-triisopropylbenzene. Catal Today. 2011;166(1):25-38.
5. Phung TK, Carnasciali MM, Finocchio E, Busca G. Catalytic conversion of ethyl acetate over faujasite zeolites. Appl Catal A Gen. 2014;470:72-80.
6. Walcarius A. Implication of zeolite chemistry in electrochemical science and applications of zeolite-modified electrodes. In: Auerbach SM, Carrado KA, Dutta PK. *Handbook of zeolite*

science and technology. Boca Raton: CRC Press; 2003. p. 721-83.

7. Doménech-Carbó A. Theoretical scenarios for the electrochemistry of porous silicate-based materials: an overview. J Solid State Electrochem. 2015;19:1887-903.

8. Franus W, Wdowin M, Franus M. Synthesis and characterization of zeolites prepared from industrial fly ash. Environ Monit Assess. 2014;186:5721-9.

9. Zanin E, Scapinello J, De Oliveira M, Rambo CL, Franscescon F, Freitas L, et al. Adsorption of heavy metals from wastewater graphic industry using clinoptilolite zeolite as adsorbent. Process Saf Environ Prot. 2017;105:194-200.

10. Wen J, Yi Y, Zeng G. Effects of modified zeolite on the removal and stabilization of heavy metals in contaminated lake sediment using BCR sequential extraction. J Environ Manage. 2016;178:63-9.

11. Muenpol S, Yuwapornpanit R, Jitkarnka S. Valuable petrochemicals, petroleum fractions, and sulfur compounds in oils derived from waste tyre pyrolysis using five commercial zeolites as catalysts: impact of zeolite properties. Clean Technol Environ Policy. 2015;17:1149-59.

12. Vogt ET, Weckhuysen BM. Fluid catalytic cracking: recent developments on the grand old lady of zeolite catalysis. Chem Soc Rev. 2015;44(20):7342-70.

13. Morris RE, Nachtigall P. Zeolites in catalysis: properties and applications. Royal Society of Chemistry; 2017.

14. Chokkareddy R, Bhajanthri NK, Redhi GG. An enzyme-induced novel biosensor for the sensitive electrochemical determination of isoniazid. Biosensors (Basel). 2017;7(2):21.

15. Balasubramanian P, Thirumalraj B, Chen SM, Barathi P. Electrochemical determination of isoniazid using gallic acid supported reduced graphene oxide. J Electrochem Soc. 2017;164(7):H503.

16. Absalan G, Akhond M, Soleimani M, Ershadifar H. Efficient electrocatalytic oxidation and determination of isoniazid on carbon ionic liquid electrode modified with electrodeposited palladium nanoparticles. J Electroanal Chem (Lausanne). 2016;761:1-7.

17. Hu YQ, Zhang S, Zhao F, Gao C, Feng LS, Lv ZS, et al. Isoniazid derivatives and their anti-tubercular activity. Eur J Med Chem. 2017;133:255-67.

18. Fang PF, Cai HL, Zhu RH, Tan QY, Gao W, Xu P, et al. Simultaneous determination of isoniazid, rifampicin, levofloxacin in mouse tissues and plasma by high performance liquid chromatography–tandem mass spectrometry. J Chromatogr B Analyt Technol Biomed Life Sci. 2010;878(24):2286-91.

19. Liu J, Zhou W, You T, Li F, Wang E, Dong S. Detection of hydrazine, methylhydrazine, and isoniazid by capillary electrophoresis with a palladium-modified microdisk array electrode. Anal Chem. 1996;68(19):3350-3.

20. Lapa RA, Lima JL, Santos JL. Fluorimetric determination of isoniazid by oxidation with cerium (IV) in a multicommutated flow system. Anal Chim Acta. 2000;419(1):17-23.

21. Haghighi B, Bozorgzadeh S. Flow injection chemiluminescence determination of isoniazid using luminol and silver nanoparticles. Microchem J. 2010;95(2):192-7.

22. Azad UP, Prajapati N, Ganesan V. Selective determination of isoniazid using bentonite clay modified electrodes. Bioelectrochemistry. 2015;101:120-5.

23. Demirkaya-Miloglu F, Oznuluer T, Ozdurak B, Miloglu E. Design and optimization of a new voltammetric method for determination of isoniazid by using PEDOT modified gold electrode in pharmaceuticls. Iranian Journal of Pharmaceutical Research: IJPR. 2016;15:65.

24. Si X, Jiang L, Wang X, Ding Y, Luo L. Determination of isoniazid content via cysteic acid/graphene modified glassy carbon electrode. Anal Methods. 2015;7(2):793-8.

25. Núñez C, Arancibia V, Triviño JJ. A new strategy for the modification of a carbon paste electrode with carrageenan hydrogel for a sensitive and selective determination of arsenic in natural waters. Talanta. 2018;187:259-64.

26. Li CM, Hu W. Electroanalysis in micro-and nano-scales. J Electroanal Chem (Lausanne). 2013;688:20-31.

27. Magossi MS, Fernandes DS, Franco FS, Felipe AS, De Vicente FS, Do Carmo DR. Inorganofunctionalization of Ti (IV) and Zr (IV) on the MCM-41 surface and its interaction with a mixed valence complex to use as isoniazid sensing. J Inorg Organomet Polym Mater. 2021;31(10):4093-102.

28. Magossi MS, Maraldi VA, Magossi MS, Dias Filho NL, Do Carmo DR. Silica gel functionalized with 4-Amino-5-(4pyridyl)-4H-1, 2, 4-triazole-3-thiol and their use as a copper sorbent and electromediator for voltammetric detection of ascorbic acid. Electroanalysis. 2018;30(11):2660-7.

29. Liu Y, Yan C, Qiu X, Li D, Wang H, Alshameri A. Preparation of faujasite block from fly ash-based geopolymer via in-situ hydrothermal method. J Taiwan Inst Chem Eng. 2016;59:433-9.

30. Zhou C, Alshameri A, Yan C, Qiu X, Wang H, Ma Y. Characteristics and evaluation of synthetic 13X zeolite from Yunnan's natural halloysite. J Porous Mater. 2013;20:587-94.

31. Chen LF, Noreña LE, Navarrete J, Wang JA. Improvement of surface acidity and structural regularity of Zr-modified mesoporous MCM-41. Mater Chem Phys. 2006;97(2-3):236-42.

32. Deng K, Li C, Qiu X, Zhou J, Hou Z. Electrochemical preparation, characterization and application of electrodes modified with nickel–cobalt hexacyanoferrate/graphene oxide–carbon nanotubes. J Electroanal Chem (Lausanne). 2015;755:197-202.

33. Do Carmo DR, Maraldi VA, Cumba LR. Voltammetric properties of nickel Hexacyanoferrate (III) obtained on the titanium (IV) Silsesquioxane occluded into the H-FAU zeolite for detection of sulfite. Silicon. 2019;11:267-76.

34. Liu Y, Yan C, Qiu X, Li D, Wang H, Alshameri A. Preparation of faujasite block from fly ash-based geopolymer via in-situ hydrothermal method. J Taiwan Inst Chem Eng. 2016;59:433-9.

35. Zhou C, Alshameri A, Yan C, Qiu X, Wang H, Ma Y. Characteristics and evaluation of synthetic 13X zeolite from Yunnan's natural halloysite. J Porous Mater. 2013;20:587-94.

36. Chen LF, Noreña LE, Navarrete J, Wang JA. Improvement of surface acidity and structural regularity of Zr-modified mesoporous MCM-41. Mater Chem Phys. 2006;97(2-3):236-42.

37. Bagkar N, Gangul R, Choudhury S, Hassan PA, Sawant S, Yakhmi JV. Synthesis of surfactant encapsulated nickel hexacyanoferrate nanoparticles and deposition of their Langmuir–Blodgett film. J Mater Chem. 2004;14:1430-6.

38. Silverstein RM, Bassler GC. Spectrometric identification of organic compounds. J Chem Educ. 1962;39(11):546.

39. Satyanarayana M, Reddy KK, Gobi KV. Multiwall carbon nanotube ensembled biopolymer electrode for selective determination of isoniazid in vitro. Anal Methods. 2014;6(11):3772-8.

40. Thommes M, Kaneko K, Neimark AV, Olivier JP, Rodriguez-Reinoso F, Rouquerol J, et al. Physisorption of gases, with special reference to the evaluation of surface area and pore size distribution (IUPAC Technical Report). Pure Appl Chem. 2015;87(9-10):1051-69.

41. Gu J, Lin J, Smith AJ, Soontaranon S, Rugmai S, Kongmark C, et al. Towards understanding mesopore formation in zeolite Y crystals using alkaline additives via in situ small-angle X-ray scattering. Microporous Mesoporous Mater. 2022;338:111867.

42. Asadpour-Zeynali K, Baghalabadi V. Electrocatalytic determination of isoniazid by a glassy carbon electrode modified with poly (Eriochrome Black T). Analytical and Bioanalytical Chemistry Research. 2017;4(1):31-40.

43. Asadpour-Zeynali K, Arteshi Y. Electroanalytical determination of isoniazid in pharmaceutical formulation and human plasma, using a poly (eriochrome black-T) modified pencil lead electrode. Iranian Journal of Analytical Chemistry. 2017;4(1):51-8.

Behaviour of the Faujasite Zeolite Occluded with Ti(IV) and Zr(IV) and its Interaction with Nickel
Hexacyanoferrate (III): A Comparative Study in the Voltammetric Detection of Isoniazid

11

44. Barbosa PFP, Andrade RDA, Vieira EG, Do Carmo DR. An intervalence complex on chitosan surface and its application for isoniazid detection in synthetic samples. Solid State Sci. 2020;104:106204.

45. Zhang Y, Jiang X, Zhang J, Zhang H, Li Y. Simultaneous voltammetric determination of acetaminophen and isoniazid using MXene modified screen-printed electrode. Biosens Bioelectron. 2019;130:315-21.

46. Couto RA, Lima JL, Quinaz MB. Screen-printed electrode based electrochemical sensor for the detection of isoniazid in pharmaceutical formulations and biological fluids. Int J Electrochem Sci. 2015;10(10):8738-49.